

UCLA

UCLA Previously Published Works

Title

Serine Protease Activation Essential for Endothelial-Mesenchymal Transition in Vascular Calcification

Permalink

<https://escholarship.org/uc/item/7dt9m3sk>

Journal

Circulation Research, 117(9)

ISSN

0009-7330

Authors

Yao, Jiayi
Guihard, Pierre J
Blazquez-Medela, Ana M
et al.

Publication Date

2015-10-09

DOI

10.1161/circresaha.115.306751

Peer reviewed



Published in final edited form as:

Circ Res. 2015 October 9; 117(9): 758–769. doi:10.1161/CIRCRESAHA.115.306751.

Serine Protease Activation Essential for Endothelial-Mesenchymal Transition in Vascular Calcification

Jiayi Yao^{1,2}, Pierre J. Guihard¹, Ana M. Blazquez-Medela¹, Yina Guo¹, Jeremiah H. Moon¹, Medet Jumabay¹, Kristina I. Boström^{1,3}, and Yucheng Yao¹

¹Division of Cardiology, David Geffen School of Medicine at UCLA, Los Angeles, CA 90095-1679, U.S.A.

²Department of Cell Biology and Genetics, School of Basic Medical Sciences, Xi'an Jiaotong University Health Science Center, 76 Western Yanta Road, Xi'an 710061, China

³The Molecular Biology Institute at UCLA, Los Angeles, CA 90095-1570, U.S.A.

Abstract

Rationale—Endothelial cells have the ability to undergo endothelial-mesenchymal transitions (EndMTs), by which they acquire a mesenchymal phenotype and stem-cell like characteristics. We previously found that EndMTs occurred in the endothelium deficient in matrix Gla protein (MGP) enabling endothelial cells to contribute cells to vascular calcification. However, the mechanism responsible for initiating EndMTs is not fully understood.

Objective—To determine the role of specific serine proteases and sex determining region Y-box 2 (Sox2) in the initiation of EndMTs.

Methods and Results—In this study, we used *in vivo* and *in vitro* models of vascular calcification to demonstrate that serine proteases and Sox2 are essential for the initiation of EndMTs in MGP-deficient endothelium. We showed that expression of a group of specific serine proteases was highly induced in endothelial cells at sites of vascular calcification in *Mgp* null aortas. Treatment with serine protease inhibitors decreased both stem-cell marker expression and vascular calcification. In human aortic endothelial cells, this group of serine proteases also induced EndMTs, and the activation of proteases was mediated by Sox2. Knockdown of the serine proteases or Sox2 diminished EndMTs and calcification. Endothelial-specific deletion of Sox2 decreased expression of stem-cell markers and aortic calcification in MGP-deficient mice.

Conclusions—Our results suggest that Sox2-mediated activation of specific serine proteases is essential for initiating EndMTs, and thus, may provide new therapeutic targets for treating vascular calcification.

Keywords

Endothelium; progenitor cell; calcification; matrix Gla protein; serine protease

Address correspondence to: Dr. Yucheng Yao, Division of Cardiology, David Geffen School of Medicine at UCLA, Box 951679, Los Angeles, CA 90095-1679, Tel: 310-825-3239, Fax: 310-206-8553, yyao@mednet.ucla.edu.

DISCLOSURES

The authors have declared that no conflict of interest exists.

INTRODUCTION

Transition of endothelial cells into mesenchymal cells (endothelial-mesenchymal transition, EndMT) allows endothelial cells (ECs) to acquire plasticity and to participate in embryonic development and disease progression¹. During embryonic development, the microenvironment or specific factors induce EndMT, driving the endothelium to engage in normal tissue differentiation^{2–5}. In disease, the occurrence of EndMTs may convert endothelium into a multipotent state that contributes cells toward undesirable differentiation such as cardiac and renal fibrosis, cancer progression, fibrodysplasia ossificans progressiva (FOP), pulmonary hypertension, and vascular calcification^{6–13}.

Vascular calcification is a frequent and severe complication of vascular disease, which increases morbidity and mortality in diabetes and atherosclerosis, and is associated with an increased risk of congestive heart failure, myocardial infarction, systemic hypertension, and chronic kidney disease^{14–18}. Previously considered to be a passive process of mineral precipitation, vascular calcification is now known to be an active process that involves ectopic bone formation^{18–20}.

Mice lacking matrix Gla protein (MGP), an inhibitor of bone morphogenetic protein (BMP)-2, 4 and 7, is a well-known model for vascular calcification²¹. The lack of MGP activates BMP signaling throughout the vascular wall²² and is associated with ectopic osteochondrogenic differentiation, vascular calcification, and EndMTs^{11, 21}. However, the mechanism by which EndMT is initiated in the calcifying arteries has not been determined. Here, we show critical roles for endothelial specific serine proteases and sex determining region Y-box 2 (Sox2) in the activation of EndMTs. Reduction of proteases activity or Sox2 levels limits EndMTs and vascular calcification.

METHODS

See Online Data Supplement for detailed Methods section.

Animals

Mgp^{+/-} mice on the C57BL/6J background²³ were obtained from Dr. Cecilia Giachelli, University of Washington, with the permission of Dr. Gerard Karsenty, Columbia University. *Cdh5*^{Cre} (B6.Cg-Tg(Cdh5-cre)7Mlia/J) and *Sox2*^{flox/flox} (*Sox2*^{tm1.1Lan/J}) mice were obtained from the Jackson Laboratory. Genotypes were confirmed by PCR^{21, 24, 25}, and experiments were performed with generations F4–F6. Littermates were used as wild type controls. All mice were fed a standard chow diet (Diet 8604, HarlanTeklad Laboratory). The studies were reviewed and approved by the Institutional Review Board and conducted in accordance with the animal care guideline set by the University of California, Los Angeles. The investigation conformed to the National Research Council, *Guide for the Care and Use of Laboratory Animals, Eighth Edition* (Washington, DC: The National Academies Press, 2011). Diisopropylfluorophosphate (DFP) (Sigma-Aldrich) and serpinin (Origene) were injected via tail vein or retro-orbital injection (20–50 ng/g, daily) as in

previous studies^{26, 27}. Injections in *Mgp*^{-/-} mice were started at 2 weeks of age, and continued for 2–4 weeks.

Tissue culture and siRNA transfections

Human aortic endothelial cells (HAECs) were cultured as previously described²⁸. For treatment of HAECs, BMP-4 (40 ng/ml, R&D system), glucose (22 nmol/L, Sigma-Aldrich), DFP (300 ng/ml), serpin1 (300 ng/ml), elastase 1 (50 ng/ml, Abnova), elastase 2 (50 ng/ml, Abcam), and kallikrein 1, 5 and 6 (all 10 ng/ml, Abnova) were added as indicated in the text. Transient transfections of HAECs with siRNA (Silencer® predesigned siRNA, Ambion) were performed with Lipofectamine™2000 (Invitrogen) using 60 nM siRNA. The amount of siRNA was optimized per the manufacturer's instructions. Three separate siRNAs and scrambled siRNA with the same nucleotide content were tested. When compared with unrelated control siRNA and scrambled siRNA, the specific siRNAs resulted in an 80–95% decrease in mRNA and protein levels as determined by real-time PCR and immunoblotting, respectively. The siRNA that provided the most efficient inhibition (90–95%) was used for all experiments. Silencer® predesigned siRNAs were obtained for MGP, SMAD1, SMAD5, SMAD8, Sox2, elastase 1 and 2, and kallikrein 1, 5 and 6. The same total amount of siRNA was added when transfections with multiple siRNAs were performed.

RNA analysis

Real-time PCR analysis was performed as previously described²⁹. Glyceraldehyde 3-phosphate dehydrogenase (GAPDH) was used as a control gene²⁹. Primers and probes for mouse Sox2, Kruppel-like factor 4 (Klf4), snail family zinc finger 2 (Slug or Snail2), spinocerebellar ataxia type 1 (Sca1), cluster of differentiation (CD)10, CD44, CD71, CD90, c-kit (or CD117), N-cadherin, and all elastases and kallikreins were obtained from Applied Biosystems as part of Taqman® Gene Expression Assays.

Immunoblotting

Immunoblotting was performed as previously described³⁰. Equal amounts of cellular protein or tissue lysates were used. Blots were incubated with specific antibodies to elastase 1 (200ng/ml; Santa Cruz Biotechnology), elastase 2 (200 ng/ml; Abgent), kallikrein 1 and 6 (both 200 ng/ml; Sigma-Aldrich), kallikrein 5 (300 ng/ml; Acris Antibodies), c-kit (200 ng/ml; Cell Signaling Technology), Sca1 (200 ng/ml; Merck Millipore), CD10 (1:100; ThermoFisher), CD44 and CD90 (both 200 ng/ml; Abcam), CD71 (1:200; ThermoFisher), pSMAD1/5/8 (200ng/ml; Santa Cruz Biotechnology), Sox2, Klf4, Slug and pSMAD2/3 (all 400 ng/ml; Cell Signaling Technology) and total SMAD (400 ng/ml; Santa Cruz Biotechnology). β -Actin (1:5000 dilution; Sigma-Aldrich) was used as loading control.

Immunofluorescence

Tissue sections were fixed in 4% paraformaldehyde and processed as previously described³¹. Immunofluorescence was performed as previously described¹¹. We used specific antibodies for CD31 (Merck Millipore), vWF (Dako), Cbfa1, Osterix and elastase 1 (all from Santa Cruz Biotechnology), elastase 2 (Abgent), kallikrein 1 and 6 (Sigma-Aldrich), kallikrein 5 (Acris Antibodies), Sox2, Klf4, c-kit, Slug (all from Cell Signaling

Technology), Sca1 (Merck Millipore), CD10 and CD71 (both from ThermoFisher), N-cadherin (Life technology), CD44 and CD90 (both from Abcam). Nuclei were stained with 4',6-diamidino-2-phenylindole (DAPI, Sigma-Aldrich).

Flow cytometric analysis

Fluorescence-activated cell sorting (FACS) analysis was performed as described¹¹. The cells were stained with fluorescein isothiocyanate (FITC)-, phycoerythrin (PE)-, or Alexa Fluor 488 (AF-488)-conjugated antibodies against Sox2, VE-cadherin, elastase 1 and 2, kallikrein 1, 5, and 6. Nonspecific fluorochrome- and isotype-matched IgGs (BD Pharmingen) served as controls.

Expression profile

The total mRNA was extracted from aortic tissue and examined by Mouse Ref-8v 2.0 Expressin Bead Chip kit (Illumina). The array data was analyzed by using GenomeStudio software (Illumina). The expression profiles of all serine proteases were extracted from array data, and the heat map was generated by using GenomeStudio.

Quantification of aortic calcium

The aortic calcium was measured by using calcium assay kit (Bioassay) as previous described³².

Enzyme-linked immunosorbent assay (ELISA)

The levels of elastases and kallikreins in plasma were examined using ELISA kits, elastase 1 (Antibodies-online), elastase 2 (MyBiosource), kallikrein 1 (Abcam), kallikrein 5 (Biocompare) and kallikrein 6 (Enzo). The assays were performed as per the manufacturer's protocols.

Lentivirus infection

Lentiviral vectors containing Sox2 open reading frame (ORF) under the cytomegalovirus (CMV) promoter were obtained from Applied Biological Materials Inc. The cell infection was performed as per the manufacturer's protocol.

Transmission electron microscopy and scanning electron microscopy

Transmission electron microscopy and scanning electron microscopy were performed as described¹¹.

Statistical analysis

Data were analyzed for statistical significance by ANOVA with post hoc Tukey's analysis. The analyses were performed using GraphPad Instat®, version 3.0 (GraphPad Software). Data represent mean \pm SD. $P < 0.05$ was considered significant, and experiments were performed a minimum of three times.

RESULTS

Lack of MGP causes endothelial-mesenchymal transition

To investigate EndMTs in MGP deficient endothelium, we examined lesions of aortic calcification in 4-week-old *Mgp*^{-/-} mice. We observed multiple layers of EC-like cells that appeared to have penetrated into the medial tissues and proliferated in the areas adjacent to an osteochondrogenic zone (Online Figure I). The internal elastic lamina (IEL) was undetectable and EC-like cells were oriented as if migrating from the luminal side toward the calcifying lesion (Online Figure I). We further examined the lesions using transmission electron microscopy (TEM) and scanning electron microscopy (SEM) at different time points from postnatal day 5 (P5) to P30. TEM indicated that degradation of IEL, which is in close contact with endothelium, began in the *Mgp*^{-/-} aorta as early as P5 (Figure 1a). At P15, fractures in the IEL were apparent and *Mgp*^{-/-} aortic ECs lost their normal morphology. At P30, the IEL was completely degraded, and a mixture of cells had replaced the normal aortic endothelium (Figure 1a). Abnormalities in the *Mgp*^{-/-} aortic endothelium were also observed by SEM, which showed ruptures in the endothelium at P10 that became progressively worse at P15 and P30 (Figure 1b).

To examine whether EndMTs drove the *Mgp*^{-/-} endothelium into a multipotent state, we analyzed the expression of the stem-cell markers Sox2, Klf4, c-kit, Sca1, CD10, CD44, CD71, CD90, and N-cadherin, and the typical mesenchymal marker Slug (also known as Snail2) in isolated *Mgp*^{-/-} aortic ECs at P14 and P28. We found that expression of all of these markers was upregulated (Figure 1c). We also immunostained the calcified aortic tissues using specific antibodies for these markers and for vWF, an endothelial marker. All of the stem-cell and mesenchymal markers were strongly induced in vWF positive cells, which were detected in the aortic medial layer and calcified lesional areas (Figure 1d and Online Figure II) suggesting that EndMTs occurred in the *Mgp*^{-/-} endothelium during the calcifying process.

Identification of serine proteases in EndMTs and calcification

Because of the highly degraded IEL in *Mgp*^{-/-} aortic tissues, we examined whether serine proteases were induced in these tissues. By comparing gene expression profiles of aortic tissues from wild type and *Mgp*^{-/-} mice at 4 weeks of age, we identified 5 serine proteases, elastase 1 and 2, and kallikrein 1, 5, and 6, which were highly induced in *Mgp*^{-/-} aortas (Figure 2a). Real-time PCR and immunoblotting of *Mgp*^{-/-} aortic tissue confirmed the induction of these 5 serine proteases (Figure 2b–2d).

We also analyzed elastases and kallikreins in plasma by ELISA, which showed similar protease levels in *Mgp*^{-/-} and *Mgp*^{+/+} mice (data not shown). Among isolated *Mgp*^{-/-} aortic cells, the fraction of elastase- and kallikrein-positive cells was 11–14% (Online Figure III). We performed immunohistochemistry to localize the elastase- and kallikrein-positive cells in *Mgp*^{-/-} aortic tissue. Elastase- and kallikrein-positive cells co-localized with the endothelial marker vWF (Figure 3a). The flow cytometric analysis also showed co-expression of elastases and kallikreins with the endothelial marker VE-cadherin in isolated *Mgp*^{-/-} aortic cells (Figure 3b), providing evidence that elastases and kallikreins were

induced in *Mgp*^{-/-} aortic endothelium. By way of confirmation, co-localization was not observed between kallikrein 5 and smooth muscle myosin heavy chain, nor between elastase 1 and alpha-smooth muscle actin (SMA) (Online Figure IV).

We treated *Mgp*^{-/-} mice with the serine protease inhibitors DFP and serpin1 for two weeks starting at 2 weeks of age. We found that 80% and 50% of *Mgp*^{-/-} mice were rescued by DFP and serpin1, respectively, after 6 weeks of treatment (Figure 4a). Aortic calcification in *Mgp*^{-/-} mice, as visualized by Alizarin Red staining, was dramatically decreased after the DFP and serpin1 treatments (Figure 4b). Total aortic calcium was similarly decreased (Figure 4c), suggesting that serine protease inhibitors limited the calcifying process. To determine whether DFP and serpin1 affected EndMTs, we analyzed the expression of stem-cell and mesenchymal markers in aortic tissues by real-time PCR and immunoblotting. We found a significant decrease in these markers in *Mgp*^{-/-} aortic tissues after DFP and serpin1 treatments (Figure 4d), suggesting that serine protease inhibitors also limited EndMTs. Together, our results suggest that serine proteases play important roles in transitioning ECs to a multipotent state allowing for osteochondrogenic differentiation.

Complexes of serine proteases induce EndMTs

To determine if the complexes of elastases and kallikreins induce EndMTs, we used HAECs, more than 99.5% of which were CD31 positive¹¹. We depleted MGP by siRNA transfection, which decreased MGP expression to <10% of normal levels after 20 to 24 hours³⁰. We combined siRNA transfection with treatment of the cells with BMP-4 (40 ng/mL) or high glucose (22 nmol/L), which strongly induces BMP expression in ECs^{11, 22}. The results showed that expression of elastase 1, 2 and kallikrein 1, 5, 6 increased with both MGP depletion and the two treatments (Online Figure V). Combined transfection of siRNA to SMAD1, 5 and 8, however, abolished the induction (Figure 5a), suggesting that elastases and kallikreins were induced by BMP signaling. We also found that expression of stem-cell and mesenchymal markers were induced in MGP-depleted HAECs (Figure 5b). We then transfected MGP-depleted HAECs treated with BMP-4 and glucose with siRNA to elastase 1, 2 and kallikrein 1, 5, 6. Depletion of the elastases and kallikreins abolished the induction of stem-cell and mesenchymal markers in MGP-depleted HAECs, and addition of BMP-4 or glucose failed to restore the expression (Figure 5c). Addition of all of elastase 1, 2 and kallikrein 1, 5, 6 induced the expression of stem-cell and mesenchymal markers in HAECs after 24 hours of treatment (Online Figure VI). We tested the addition of individual elastases, kallikreins and various combinations; only the combination of all five proteases affected the marker expression (data not shown). We examined the progenitor capacity of HAECs undergoing EndMTs. We transfected HAECs with MGP siRNA and treated with glucose and BMP-4, or treated with serine proteases. We examined the proliferative activity, and found increased proliferation in MGP-depleted HAECs. The increase was enhanced by BMP-4 and glucose (Online Figure VIIa). We examined colony-forming unit fibroblast (CFU-F) ability by alkaline phosphatase staining, and found that the CFU-F was higher in MGP-depleted or serine proteases treated HAECs (Online Figure VIIb). We also treated cells with adipogenic, cardiomyogenic or neurogenic medium. After 7 days of treatment, we examined the expression of adipogenic markers (peroxisome proliferator-activated receptor gamma, PPARgamma and CCAAT/enhancer-binding protein beta, C/EBPβ), cardiomyocyte

markers (NK2 homeobox 5, Nkx2.5, and Troponin I), and neuronal markers (nestin and neuroD) by real-time PCR. All these markers were increased in the MGP-depleted or serine proteases treated HAECs (Online Figure VIIc–d). The results suggested that HAECs gained multipotency after MGP-depletion or treatment with serine proteases. Together, the results suggested that EndMTs are activated by complexes of elastases and kallikreins induced by BMP signaling in the endothelium.

Induction of Sox2-mediated mesenchymal transitions

To identify factors that mediate activation of EndMTs by elastases and kallikreins, we focused on the highly induced stem-cell markers that included both transcription factors and cell surface receptors. We depleted the expression of Sox2, Klf4, c-kit, Slug, Sca1, CD10, CD44, CD71 and CD90 individually in HAECs (using specific siRNA), and treated with elastase and kallikrein. Immunoblotting showed that depletion of Sox2 abolished the induction of all other markers (Figure 6a). We then used Sox2-expressing lentivirus to restore Sox2 in HAECs depleted of MGP, elastases, and kallikreins, and treated the cells with BMP-4 and high glucose. Immunoblotting showed a re-emergence of stem-cell and mesenchymal markers in HAECs after restoration of Sox2 (Online Figure VIII). We also restored Sox2 in MGP-depleted HAECs treated with DFP and serpin1, which similarly led to the re-emergence of stem-cell and mesenchymal markers (Figure 6b). These results suggested that Sox2 mediated EndMTs after depletion of MGP.

To examine the effects of elastases, kallikreins, and Sox2 on osteogenic differentiation in MGP-depleted HAECs, we depleted MGP, elastases, and kallikreins, and then treated the cells for 4 days with osteogenic medium alone, osteogenic medium with BMP-2 (200 ng/mL) and high glucose (22 nmol/L), or a combination of osteogenic medium with either BMP-2 or glucose starting the day after siRNA transfection. Immunoblotting showed that with all four treatments, expression of the osteogenic markers Cbfa1 and Osterix was increased when MGP was depleted, but when elastases and kallikreins were knocked down, the expression of osteogenic markers was abolished (Figure 6c). Depletion of Sox2 also inhibited induction of Cbfa1 and Osterix in MGP-depleted HAECs in the same type of experiment (Figure 6d). Mineral staining (Alizarin Red and Von Kossa) confirmed that depletion of elastases and kallikreins or Sox2 limited calcium accumulation in MGP-depleted HAECs after 7 and 14 days of treatment (Figure 5e–f).

Endothelial-specific deletion of Sox2 decreases aortic calcification

We examined if Sox2 co-localized with proteases and Cbfa1 in vivo using immunofluorescence. Elastase 1, 2 and kallikrein 1, 5, 6 all co-localized with Sox2 and Cbfa1 in aortic endothelium of *Mgp*^{-/-} mice at 4 weeks of age (Figure 7a and Online Figure IX). We pre-sorted VE-cadherin+CD45⁻ aortic ECs from aortic tissues; CD45⁺ cells, which may represent CD31⁺ leukocyte populations, were excluded. Flow cytometric analysis showed that more than 30% of aortic ECs co-expressed elastases and kallikreins together with Sox2 (Online Figure X). These results suggested that the induction of Sox2 expression in ECs is caused by induction of elastases and kallikreins.

To determine if a cell-specific decrease of Sox2 in endothelium would limit EndMTs and vascular calcification, we crossed *Cdh5^{Cre}* and *Sox2^{Flox/Flox}* mice with *Mgp^{+/-}* mice to selectively reduce Sox2 by Cre-mediated deletion in ECs by Cdh5 (VE-cadherin)-driven Cre expression. We examined the aortas of *Cdh5^{Cre}Sox2^{Flox/wt}Mgp^{-/-}* mice at 4 weeks of age and found that expression of Sox2 was decreased in the aortic endothelium (Figure 7b). Immunoblotting showed that expression of stem-cell and mesenchymal markers were significantly decreased in the aortic endothelium of *Cdh5^{Cre}Sox2^{Flox/wt}Mgp^{-/-}* mice (Figure 7c). Total aortic calcium was significantly reduced (Figure 7d) and Alizarin Red staining of whole aortic tissues showed a decrease in aortic mineralization in *Cdh5^{Cre}Sox2^{Flox/wt}Mgp^{-/-}* mice (Figure 7e). This suggested that EndMTs and vascular calcification are limited by endothelial Sox2 reduction.

We further examined the expression of elastase 1, 2 and kallikrein 1, 5, 6 in aortas of *Cdh5^{Cre}Sox2^{Flox/wt}Mgp^{-/-}* mice by real-time PCR. We found decreased expression of all the five serine proteases (Figure 7f), suggesting that reducing Sox2 in *Mgp^{-/-}* endothelium decreased the induction of serine proteases.

Mutual regulation of Sox2 and Twist1 in EndMTs in vascular calcification

Twist1 is known to induce osteogenesis and play important roles in EndMTs and in epithelial-mesenchymal transitions³³⁻³⁵, where Twist1 and Sox2 were also shown to regulate each other³⁶. To determine if Twist1 plays a role in EndMTs in *Mgp^{-/-}* aortas, we examined the expression of Twist1 in presorted VE-cadherin+CD45- aortic ECs from 4-week-old *Mgp^{-/-}* mice by real-time PCR, and found it to be increased (Figure 8a). We co-stained Twist1 with the endothelial marker vWF, which showed that Twist1 co-localized with vWF in *Mgp^{-/-}* aortas (Figure 8b). We also examined expression of Twist1 in MGP-depleted HAECs, and similarly found it to be increased. The induction of Twist1 was enhanced by treatment of BMP-4 and glucose, and abolished by depletion of Sox2 (Figure 8c). We then depleted Twist1 in MGP-depleted HAECs, treated with BMP-4 and glucose, and examined the stem-cell markers Sox2, Klf4 and c-kit. The depletion of Twist1 decreased induction of Sox2, Klf4 and c-kit (figure 8d), suggesting that Twist1 and Sox2 are able to mutually regulate each other during the initiation of EndMTs in MGP-depleted HAECs.

Furthermore, we depleted MGP and Twist1, and treated the cells for 4 days with osteogenic medium with either BMP-2 or glucose starting the day after siRNA transfection. The results showed that depletion of Twist1 abolished the induction of Cbfa1 and Osterix in MGP-depleted HAECs (Figure 8e). Altogether, the results suggested that Twist1 cooperated with Sox2 and played a role in initiating EndMTs leading to calcification.

DISCUSSION

Our results suggest that lack of MGP, a BMP inhibitor, results in the induction of endothelial elastases and kallikreins. The proteolytic activation of the elastases and kallikreins is instrumental in initiating EndMTs via a process mediated by Sox2, and allows for the emergence of multipotency and ultimately vascular calcification. Other studies have shown that elastases and kallikreins play important roles in vascular development and diseases, such as remodeling of the brachial artery and pulmonary hypertension³⁷⁻³⁹. Our

results expand the role of serine proteases to the transition of ECs into stem-cell like cells, suggesting that tight regulation of these enzymes is important for the maintenance of endothelial stability and differentiation.

In our experiments, all five serine proteases had to be combined to induce mesenchymal stem-cell markers. Any combination with fewer serine proteases failed to initiate EndMTs. Elastase 1 and 2, and kallikrein 1, 5 and 6 all have chymotrypsin-like specificities, but because of different structures, the cleavage of various protein substrates differs^{40, 41}. Under MGP-deficient conditions, it is possible that these proteases modify the endothelial microenvironment allowing the ECs to adopt a different cell fate.

Vascular calcification is a common complication of diabetic vasculopathy and atherosclerosis, and levels of elastases and kallikreins are elevated in diabetic patients as well as in atherosclerotic lesions^{42, 43}. Our observations point toward new ways of explaining vascular calcification in these conditions and may lead to new strategies for limiting calcification.

Endothelial Sox2 was instrumental in the activation of EndMTs in HAECs. As an essential factor for development and somatic cell reprogramming, Sox2 acts as a key factor in cell fate determination⁴⁴. Previous studies have shown that Sox2 plays a role in epithelial-mesenchymal transition in neural crest development and cancer^{45, 46}. It has also been reported that fibroblasts exhibit mesenchymal phenotypes after infection with Sox2 lentiviral vectors^{47, 48}. Our findings broaden the functions of Sox2 to also include activation of EndMTs in the aortic endothelium.

Our observation that serine proteases induce Sox2 also provides new information applicable to development. Expression of Sox2 is sustained along the ectoderm, where organs emerge from interactions between the epithelium and the mesenchyme⁴⁹, and proteolytic activity appears to be induced in tissue development⁵⁰⁻⁵². Based on our data, it is possible that serine proteases regulate Sox2 to modulate mutual transitions of the endothelium and the mesenchyme to achieve correct cell differentiation as well as coordination between tissue-specific elements and the vasculature.

In our study, BMP-4 acted as an inductive factor of EndMTs in MGP deficiency, which is consistent with results from other investigators^{6, 53}. The BMPs elicit their activity through ligand-initiated heterodimerization of BMP type II receptors (BMPRII) and type I receptors referred to as activin receptor-like kinase (ALK) 1, 2, 3, and 6⁵⁴. Activation of the type I receptor by BMPRII leads to phosphorylation of a series of SMAD proteins, which mediate the gene regulation⁵⁴. Our previous studies in HAECs showed that the same glucose treatment used to induce EndMTs also enhanced expression of BMPRII²². Interestingly, it has been shown that EndMTs associated with pulmonary arterial hypertension occur when the BMPRII levels are reduced^{34, 55}. Therefore, we also examined the expression of stem-cell markers in *Mgp*^{-/-} lungs, and the effect of MGP-deficiency, BMP-4, glucose, and serine proteases on EndMTs in cultured human pulmonary artery ECs (HPAECs). To our surprise, we found no evidence of enhanced stem-cell marker expression or EndMTs in the *Mgp*^{-/-} lungs or the HPAECs (unpublished observations), strongly suggesting that the

pulmonary arteries differ in their response to MGP deficiency. This is further supported by the finding that MGP-deficiency causes arteriovenous malformations (AVMs) rather than vascular calcification in the pulmonary circulation³⁰. Indeed, tissue-specific ECs from various organs have been reported to have unique signatures of gene expression, and to differ in their responses to stimulus⁵⁶. In addition, we have observed different responses to MGP-deficiency in the pulmonary and cerebral vascular beds. VEGF is enhanced in the pulmonary vasculature, whereas Notch signaling is enhanced in cerebral vasculature, even though in both cases, MGP-deficiency leads to AVMs^{30, 57}.

The response to loss of BMPRII may be difficult to predict, since BMPRII has been shown to be a target of multiple pro-inflammatory factors⁵⁸, and absence of BMPRII might allow for enhanced BMP6/7 signaling through recruitment of the activin type II receptor⁵⁹. Another complicating factor is that different BMP and TGF β ligands affect EndMTs differently. Whereas BMP-4 enhances EndMTs, BMP-2 and -7 have been reported to reverse EndMTs induced by TGF β 1⁵⁵. TGF β 1 elicits its activity through ALK5, which is induced by BMP-4 in HAECs³⁰, suggesting that TGF β 1-mediated EndMTs might still be regulated by BMP-4 depending on the type of endothelium. In addition, excess BMP-2 and -7 might compete with BMP-4 for binding to the same BMP receptors, thereby altering the balance that promotes or reverses EndMTs.

Previous studies have shown increased alpha-SMA expression in ECs undergoing EndMTs in pulmonary hypertension³⁴. In addition, we showed increased expression of alpha-SMA and SM22alpha in EC-like cells in the media of *Mgp*^{-/-} aortas¹¹, further supporting that these early SMC markers are expressed in transitioning ECs. Speer et al.²¹ demonstrated by lineage-tracing that SM22alpha positive cells contribute to osteochondrogenic differentiation in *Mgp*^{-/-} aortas, although it is not clear if a fraction of these cells might have been derived from the endothelium.

Smooth muscle cells (SMCs) reside in the vascular media, which is separated from the endothelium by the IEL. As the IEL is degraded, the SMCs are likely to be exposed to endothelial signaling, matrix alterations, and other effects of increased serine protease activity. This may affect the SMC phenotype and contribute to vascular calcification.

During development, expression of VE-cadherin is detected in ECs as well as in hematopoietic cells that arise from the hemogenic endothelium of the dorsal aortas⁶⁰. Therefore, we cannot rule out a contribution to the observed phenotype from altered Sox2 signaling in hematopoietic cells. However, we have previously shown that expression of inflammatory and monocyte markers is minimal or undetectable in *Mgp*^{-/-} aortas⁶¹. Thus it is less likely that hematopoietic cells, such as monocytes, would directly transit to or affect osteoprogenitor cells in the *Mgp*^{-/-} aortas. Furthermore, even if the exclusion of CD45+ cells prior to flow cytometric analysis of the *Mgp*^{-/-} aortic cells removed CD45+C31+ leukocytic cells, 20–30% of the analyzed ECs still co-expressed CD31 and Sox2. EC lineage tracing and co-staining of EC and multipotency or osteogenic markers in our previous studies further supported the endothelium as a source of osteogenic cells¹¹. Altogether, our results suggest an important role for Sox2 in initiating EndMTs in vascular calcification.

Supplementary Material

Refer to Web version on PubMed Central for supplementary material.

ACKNOWLEDGEMENT

Electron microscopy was performed under supervision of Sirus A. Kohan at the Electron Microscopy Services Center of UCLA Brain Research Institute.

SOURCES OF FUNDING

Funding for this work was provided in part by NIH grants NS79353, HL30568, HL81397, and HL112839, and by a grant from the American Heart Association (Western Affiliate).

Nonstandard Abbreviations and Acronyms

AVMs	Arteriovenous malformations
BMP	Bone morphogenetic protein
Cbfa1	Core binding factor alpha 1
CD	Cluster of differentiation
DFP	Diisopropylfluorophosphate
EndMT	Endothelial-mesenchymal transition
ELA	Elastase
ELISA	Enzyme-linked immunosorbent assay
FOP	Fibrodysplasia ossificans progressiva
Gla	Gamma-carboxyglutamic acid
HAEC	Human aortic endothelial cells
KLF4	Kruppel-like factor 4
KLK	Kallikrein
MGP	Matrix Gla protein
Sox2	Sex determining region Y-box 2
Sca1	Stem Cell Antigen 1
SEM	Scanning electron microscopy
pSMAD	Phosphorylated SMAD
SMAD	Homolog of the drosophila protein, mothers against decapentaplegic (MAD) and the <i>C. elegans</i> protein SMA
SMC	Smooth muscle cells
SMA	alpha-smooth muscle actin
TEM	Transmission electron microscopy

Twist1	Twist-related protein 1
vWF	von Willebrand factor
wt	wild type

REFERENCES

1. Kovacic JC, Mercader N, Torres M, Boehm M, Fuster V. Epithelial-to-mesenchymal and endothelial-to-mesenchymal transition: From cardiovascular development to disease. *Circulation*. 2012; 125:1795–1808. [PubMed: 22492947]
2. Kisanuki YY, Hammer RE, Miyazaki J, Williams SC, Richardson JA, Yanagisawa M. Tie2-cre transgenic mice: A new model for endothelial cell-lineage analysis in vivo. *Dev Biol*. 2001; 230:230–242. [PubMed: 11161575]
3. Kirby ML, Gale TF, Stewart DE. Neural crest cells contribute to normal aorticopulmonary septation. *Science*. 1983; 220:1059–1061. [PubMed: 6844926]
4. Manner J. Does the subepicardial mesenchyme contribute myocardioblasts to the myocardium of the chick embryo heart? A quail-chick chimera study tracing the fate of the epicardial primordium. *Anat Rec*. 1999; 255:212–226. [PubMed: 10359522]
5. Gittenberger-de Groot AC, Vrancken Peeters MP, Mentink MM, Gourdie RG, Poelmann RE. Epicardium-derived cells contribute a novel population to the myocardial wall and the atrioventricular cushions. *Circ Res*. 1998; 82:1043–1052. [PubMed: 9622157]
6. Medici D, Shore EM, Lounev VY, Kaplan FS, Kalluri R, Olsen BR. Conversion of vascular endothelial cells into multipotent stem-like cells. *Nat Med*. 2010; 16:1400–1406. [PubMed: 21102460]
7. Potenta S, Zeisberg E, Kalluri R. The role of endothelial-to-mesenchymal transition in cancer progression. *Br J Cancer*. 2008; 99:1375–1379. [PubMed: 18797460]
8. Zeisberg EM, Tarnavski O, Zeisberg M, Dorfman AL, McMullen JR, Gustafsson E, Chandraker A, Yuan X, Pu WT, Roberts AB, Neilson EG, Sayegh MH, Izumo S, Kalluri R. Endothelial-to-mesenchymal transition contributes to cardiac fibrosis. *Nat Med*. 2007; 13:952–961. [PubMed: 17660828]
9. Zeisberg EM, Potenta SE, Sugimoto H, Zeisberg M, Kalluri R. Fibroblasts in kidney fibrosis emerge via endothelial-to-mesenchymal transition. *J Am Soc Nephrol*. 2008; 19:2282–2287. [PubMed: 18987304]
10. Arciniegas E, Frid MG, Douglas IS, Stenmark KR. Perspectives on endothelial-to-mesenchymal transition: Potential contribution to vascular remodeling in chronic pulmonary hypertension. *Am J Physiol Lung Cell Mol Physiol*. 2007; 293:L1–L8. [PubMed: 17384082]
11. Yao Y, Jumabay M, Ly A, Radparvar M, Cubberly MR, Bostrom KI. A role for the endothelium in vascular calcification. *Circ Res*. 2013; 113:495–504. [PubMed: 23852538]
12. Wylie-Sears J, Aikawa E, Levine RA, Yang JH, Bischoff J. Mitral valve endothelial cells with osteogenic differentiation potential. *Arterioscler Thromb Vasc Biol*. 2011; 31:598–607. [PubMed: 21164078]
13. Xu X, Friehs I, Zhong Hu T, Melnychenko I, Tampe B, Alnour F, Iascone M, Kalluri R, Zeisberg M, Del Nido PJ, Zeisberg EM. Endocardial fibroelastosis is caused by aberrant endothelial to mesenchymal transition. *Circ Res*. 2015; 116:857–866. [PubMed: 25587097]
14. Giachelli CM. The emerging role of phosphate in vascular calcification. *Kidney Int*. 2009; 75:890–897. [PubMed: 19145240]
15. Amos AF, McCarty DJ, Zimmet P. The rising global burden of diabetes and its complications: Estimates and projections to the year 2010. *Diabet Med*. 1997; 14(Suppl 5):S1–S85. [PubMed: 9450510]
16. Luscher TF, Creager MA, Beckman JA, Cosentino F. Diabetes and vascular disease: Pathophysiology, clinical consequences, and medical therapy: Part ii. *Circulation*. 2003; 108:1655–1661. [PubMed: 14517152]

17. Wu KK, Huan Y. Diabetic atherosclerosis mouse models. *Atherosclerosis*. 2007; 191:241–249. [PubMed: 16979174]
18. Sage AP, Tintut Y, Demer LL. Regulatory mechanisms in vascular calcification. *Nat Rev Cardiol*. 2010; 7:528–536. [PubMed: 20664518]
19. Vattikuti R, Towler DA. Osteogenic regulation of vascular calcification: An early perspective. *Am J Physiol Endocrinol Metab*. 2004; 286:E686–E696. [PubMed: 15102615]
20. El-Abbadi M, Giachelli CM. Mechanisms of vascular calcification. *Adv Chronic Kidney Dis*. 2007; 14:54–66. [PubMed: 17200044]
21. Speer MY, Yang HY, Brabb T, Leaf E, Look A, Lin WL, Frutkin A, Dichek D, Giachelli CM. Smooth muscle cells give rise to osteochondrogenic precursors and chondrocytes in calcifying arteries. *Circ Res*. 2009; 104:733–741. [PubMed: 19197075]
22. Bostrom KI, Jumabay M, Matveyenko A, Nicholas SB, Yao Y. Activation of vascular bone morphogenetic protein signaling in diabetes mellitus. *Circ Res*. 2011; 108:446–457. [PubMed: 21193740]
23. Luo G, Ducey P, McKee MD, Pinero GJ, Loyer E, Behringer RR, Karsenty G. Spontaneous calcification of arteries and cartilage in mice lacking matrix gla protein. *Nature*. 1997; 386:78–81. [PubMed: 9052783]
24. Alva JA, Zovein AC, Monvoisin A, Murphy T, Salazar A, Harvey NL, Carmeliet P, Iruela-Arispe ML. Ve-cadherin-cre-recombinase transgenic mouse: A tool for lineage analysis and gene deletion in endothelial cells. *Dev Dyn*. 2006; 235:759–767. [PubMed: 16450386]
25. Shaham O, Smith AN, Robinson ML, Taketo MM, Lang RA, Ashery-Padan R. Pax6 is essential for lens fiber cell differentiation. *Development*. 2009; 136:2567–2578. [PubMed: 19570848]
26. Stoller JK, Aboussouan LS. Alpha1-antitrypsin deficiency. *Lancet*. 2005; 365:2225–2236. [PubMed: 15978931]
27. Lin T, Duek O, Dori A, Kofman O. Differential long term effects of early diisopropylfluorophosphate exposure in balb/c and c57bl/j6 mice. *Int J Dev Neurosci*. 2012; 30:113–120. [PubMed: 22197972]
28. Yao Y, Zebboudj AF, Shao E, Perez M, Bostrom K. Regulation of bone morphogenetic protein-4 by matrix gla protein in vascular endothelial cells involves activin-like kinase receptor 1. *J Biol Chem*. 2006; 281:33921–33930. [PubMed: 16950789]
29. Bostrom K, Zebboudj AF, Yao Y, Lin TS, Torres A. Matrix gla protein stimulates vegf expression through increased transforming growth factor-beta1 activity in endothelial cells. *J Biol Chem*. 2004; 279:52904–52913. [PubMed: 15456771]
30. Yao Y, Jumabay M, Wang A, Bostrom KI. Matrix gla protein deficiency causes arteriovenous malformations in mice. *J Clin Invest*. 2011; 121:2993–3004. [PubMed: 21765215]
31. Jumabay M, Abdmaulen R, Urs S, Heydarkhan-Hagvall S, Chazenbalk GD, Jordan MC, Roos KP, Yao Y, Bostrom KI. Endothelial differentiation in multipotent cells derived from mouse and human white mature adipocytes. *J Mol Cell Cardiol*. 2012; 53:790–800. [PubMed: 22999861]
32. Yao Y, Bennett BJ, Wang X, Rosenfeld ME, Giachelli C, Luscis AJ, Bostrom KI. Inhibition of bone morphogenetic proteins protects against atherosclerosis and vascular calcification. *Circ Res*. 2012; 107:485–494. [PubMed: 20576934]
33. Yuen HF, Kwok WK, Chan KK, Chua CW, Chan YP, Chu YY, Wong YC, Wang X, Chan KW. Twist modulates prostate cancer cell-mediated bone cell activity and is upregulated by osteogenic induction. *Carcinogenesis*. 2008; 29:1509–1518. [PubMed: 18453541]
34. Ranchoux B, Antigny F, Rucker-Martin C, Hautefort A, Pechoux C, Bogaard HJ, Dorfmueller P, Remy S, Lecerf F, Plante S, Chat S, Fadel E, Houssaini A, Anegon I, Adnot S, Simonneau G, Humbert M, Cohen-Kaminsky S, Perros F. Endothelial-to-mesenchymal transition in pulmonary hypertension. *Circulation*. 2015; 131:1006–1018. [PubMed: 25593290]
35. Yang MH, Hsu DS, Wang HW, Wang HJ, Lan HY, Yang WH, Huang CH, Kao SY, Tzeng CH, Tai SK, Chang SY, Lee OK, Wu KJ. *Bmi1* is essential in *twist1*-induced epithelial-mesenchymal transition. *Nat Cell Biol*. 2010; 12:982–992. [PubMed: 20818389]
36. Velpula KK, Dasari VR, Tsung AJ, Dinh DH, Rao JS. Cord blood stem cells revert glioma stem cell emt by down regulating transcriptional activation of *sox2* and *twist1*. *Oncotarget*. 2011; 2:1028–1042. [PubMed: 22184289]

37. Yayama K, Kunimatsu N, Teranishi Y, Takano M, Okamoto H. Tissue kallikrein is synthesized and secreted by human vascular endothelial cells. *Biochim Biophys Acta*. 2003; 1593:231–238. [PubMed: 12581867]
38. Aimes RT, Zijlstra A, Hooper JD, Ogbourne SM, Sit ML, Fuchs S, Gotley DC, Quigley JP, Antalis TM. Endothelial cell serine proteases expressed during vascular morphogenesis and angiogenesis. *Thromb Haemost*. 2003; 89:561–572. [PubMed: 12624642]
39. Azizi M, Boutouyrie P, Bissery A, Agharazii M, Verbeke F, Stern N, Bura-Riviere A, Laurent S, Alhenc-Gelas F, Jeunemaitre X. Arterial and renal consequences of partial genetic deficiency in tissue kallikrein activity in humans. *J Clin Invest*. 2005; 115:780–787. [PubMed: 15765151]
40. Debela M, Magdolen V, Schechter N, Valachova M, Lottspeich F, Craik CS, Choe Y, Bode W, Goettig P. Specificity profiling of seven human tissue kallikreins reveals individual subsite preferences. *J Biol Chem*. 2006; 281:25678–25688. [PubMed: 16740631]
41. Paliouras M, Diamandis EP. The kallikrein world: An update on the human tissue kallikreins. *Biol Chem*. 2006; 387:643–652. [PubMed: 16800725]
42. Campbell DJ, Kladis A, Zhang Y, Jenkins AJ, Prior DL, Yii M, Kenny JF, Black MJ, Kelly DJ. Increased tissue kallikrein levels in type 2 diabetes. *Diabetologia*. 2010; 53:779–785. [PubMed: 20225398]
43. Antonicelli F, Bellon G, Debelle L, Hornebeck W. Elastin-elastases and inflamm-aging. *Curr Top Dev Biol*. 2007; 79:99–155. [PubMed: 17498549]
44. Sarkar A, Hochedlinger K. The sox family of transcription factors: Versatile regulators of stem and progenitor cell fate. *Cell Stem Cell*. 2013; 12:15–30. [PubMed: 23290134]
45. Mandalos N, Rhinn M, Granchi Z, Karampelas I, Mitsiadis T, Economides AN, Dolle P, Remboutsika E. Sox2 acts as a rheostat of epithelial to mesenchymal transition during neural crest development. *Front Physiol*. 2014; 5:345. [PubMed: 25309446]
46. Luo W, Li S, Peng B, Ye Y, Deng X, Yao K. Embryonic stem cells markers sox2, oct4 and nanog expression and their correlations with epithelial-mesenchymal transition in nasopharyngeal carcinoma. *PLoS One*. 2013; 8:e56324. [PubMed: 23424657]
47. Campolo F, Gori M, Favaro R, Nicolis S, Pellegrini M, Botti F, Rossi P, Jannini EA, Dolci S. Essential role of sox2 for the establishment and maintenance of the germ cell line. *Stem Cells*. 2013; 31:1408–1421. [PubMed: 23553930]
48. Yang N, Hui L, Wang Y, Yang H, Jiang X. Overexpression of sox2 promotes migration, invasion, and epithelial-mesenchymal transition through the wnt/beta-catenin pathway in laryngeal cancer hep-2 cells. *Tumour Biol*. 2014; 35:7965–7973. [PubMed: 24833089]
49. Pispa J, Thesleff I. Mechanisms of ectodermal organogenesis. *Dev Biol*. 2003; 262:195–205. [PubMed: 14550785]
50. Yamasaki K, Schaubert J, Coda A, Lin H, Dorschner RA, Schechter NM, Bonnart C, Descargues P, Hovnanian A, Gallo RL. Kallikrein-mediated proteolysis regulates the antimicrobial effects of cathelicidins in skin. *FASEB J*. 2006; 20:2068–2080. [PubMed: 17012259]
51. Yamakoshi Y, Hu JC, Fukae M, Yamakoshi F, Simmer JP. How do enamelysin and kallikrein 4 process the 32-kda enamelin? *Eur J Oral Sci*. 2006; 114(Suppl 1):45–51. discussion 93–45, 379–380. [PubMed: 16674662]
52. Bando Y, Ito S, Nagai Y, Terayama R, Kishibe M, Jiang YP, Mitrovic B, Takahashi T, Yoshida S. Implications of protease m/neurosin in myelination during experimental demyelination and remyelination. *Neurosci Lett*. 2006; 405:175–180. [PubMed: 16890353]
53. Malhotra R, Burke MF, Martyn T, Shakartz HR, Thayer TE, O'Rourke C, Li P, Derwall M, Spagnoli E, Kolodziej SA, Hoeft K, Mayeur C, Jiramongkolchai P, Kumar R, Buys ES, Yu PB, Bloch KD, Bloch DB. Inhibition of bone morphogenetic protein signal transduction prevents the medial vascular calcification associated with matrix gla protein deficiency. *PLoS One*. 2015; 10:e0117098. [PubMed: 25603410]
54. Miyazono K, Maeda S, Imamura T. Bmp receptor signaling: Transcriptional targets, regulation of signals, and signaling cross-talk. *Cytokine Growth Factor Rev*. 2005; 16:251–263. [PubMed: 15871923]
55. Reynolds AM, Holmes MD, Danilov SM, Reynolds PN. Targeted gene delivery of bmpr2 attenuates pulmonary hypertension. *Eur Respir J*. 2012; 39:329–343. [PubMed: 21737550]

56. Nolan DJ, Ginsberg M, Israely E, Palikuqi B, Poulos MG, James D, Ding BS, Schachterle W, Liu Y, Rosenwaks Z, Butler JM, Xiang J, Rafii A, Shido K, Rabbany SY, Elemento O, Rafii S. Molecular signatures of tissue-specific microvascular endothelial cell heterogeneity in organ maintenance and regeneration. *Dev Cell*. 2013; 26:204–219. [PubMed: 23871589]
57. Yao Y, Yao J, Radparvar M, Blazquez-Medela AM, Guihard PJ, Jumabay M, Bostrom KI. Reducing jagged 1 and 2 levels prevents cerebral arteriovenous malformations in matrix gla protein deficiency. *Proc Natl Acad Sci U S A*. 2013; 110:19071–19076. [PubMed: 24191040]
58. Kim CW, Song H, Kumar S, Nam D, Kwon HS, Chang KH, Son DJ, Kang DW, Brodie SA, Weiss D, Vega JD, Alberts-Grill N, Griendling K, Taylor WR, Jo H. Anti-inflammatory and antiatherogenic role of bmp receptor ii in endothelial cells. *Arterioscler Thromb Vasc Biol*. 2013; 33:1350–1359. [PubMed: 23559633]
59. Yu PB, Beppu H, Kawai N, Li E, Bloch KD. Bone morphogenetic protein (bmp) type ii receptor deletion reveals bmp ligand-specific gain of signaling in pulmonary artery smooth muscle cells. *J Biol Chem*. 2005; 280:24443–24450. [PubMed: 15883158]
60. Zovein AC, Hofmann JJ, Lynch M, French WJ, Turlo KA, Yang Y, Becker MS, Zanetta L, Dejana E, Gasson JC, Tallquist MD, Iruela-Arispe ML. Fate tracing reveals the endothelial origin of hematopoietic stem cells. *Cell Stem Cell*. 2008; 3:625–636. [PubMed: 19041779]
61. Yao Y, Bennett BJ, Wang X, Rosenfeld ME, Giachelli C, Lusis AJ, Bostrom KI. Inhibition of bone morphogenetic proteins protects against atherosclerosis and vascular calcification. *Circ Res*. 2010; 107:485–494. [PubMed: 20576934]

Novelty and Significance

What Is Known?

- Vascular calcification is a frequent complication of cardiovascular diseases.
- Endothelial-mesenchymal transitions (EndMTs) contribute to vascular calcification.
- Lack of matrix Gla protein (MGP), an inhibitor of bone morphogenetic proteins (BMP), induces EndMTs thereby promoting vascular calcification.

What New Information Does This Article Contribute?

- Specific serine proteases and sex determining region Y-box 2 (Sox2) are induced in endothelial cells at sites of vascular calcification in *Mgp* null aortas.
- Serine proteases are essential for the initiation of EndMTs by inducing Sox2 in MGP-deficient endothelium.
- Inhibition of serine proteases or suppression of Sox2 diminished EndMTs and vascular calcification.

Vascular calcification frequently complicates vascular diseases. EndMTs enable endothelium to contribute cells to vascular calcification. However, the initiation of EndMTs in vascular calcification is poorly understood. We report that Sox2-mediated activation of specific serine proteases is essential for initiating EndMTs. Using mouse models and cultured endothelial cells, we demonstrate that lack of the BMP-inhibitor MGP or enhanced BMP expression activates serine proteases and induces EndMTs. The activation of serine proteases is mediated by Sox2. These findings identify the serine proteases and Sox2 as the factors in EndMTs and vascular calcification and may provide therapeutic targets for treating vascular calcification.

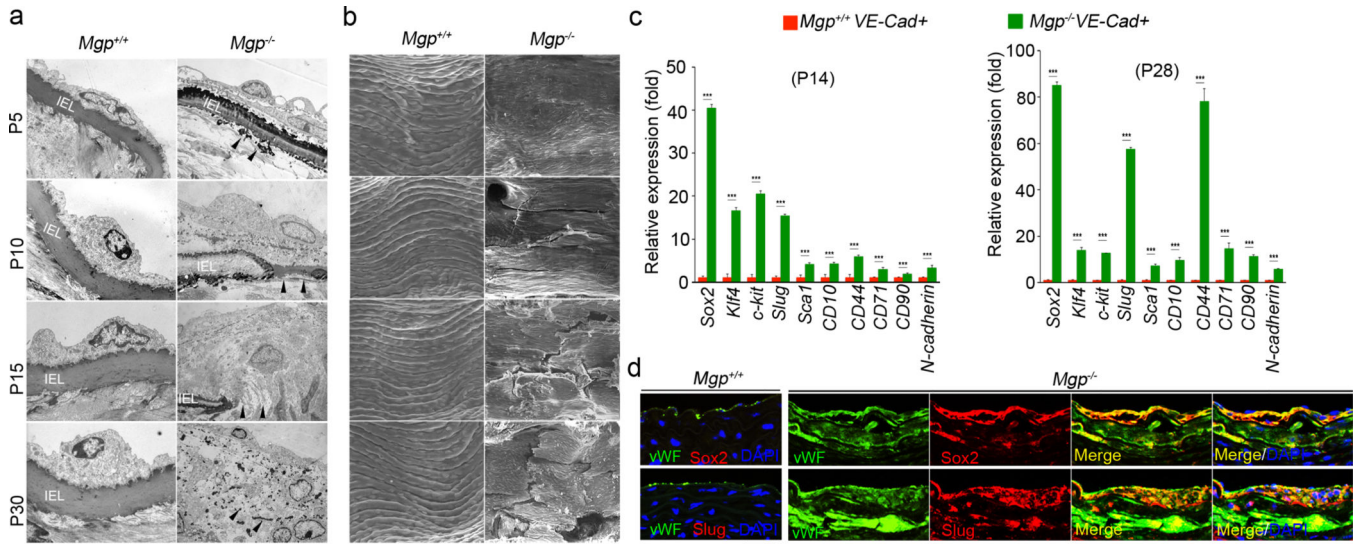


Figure 1. Lack of MGP causes EndMTs in aortic tissue

(a–b) *Mgp*^{+/+} and *Mgp*^{-/-} aortic endothelium was examined by transmission electron microscopy (TEM) (a) and scanning electron microscopy (SEM) (b). Magnification for TEM, 3.7×10^3 . Magnification for SEM, 5×10^2 . IEL: Internal elastic lamina. Areas of IEL degradation are indicated by arrowheads. (c) Expression of stem-cell and mesenchymal markers in VE-cadherin-positive and CD45-negative presorted cells from *Mgp*^{+/+} and *Mgp*^{-/-} aortas at postnatal day (P) 14 and 28, as determined by real-time PCR. *** $p < 0.001$. (d) Co-expression of the endothelial marker vWF with the stem-cell marker Sox2 and the mesenchymal marker Slug in calcified lesions of *Mgp*^{-/-} aortas. Scale bars, 100 μ m.

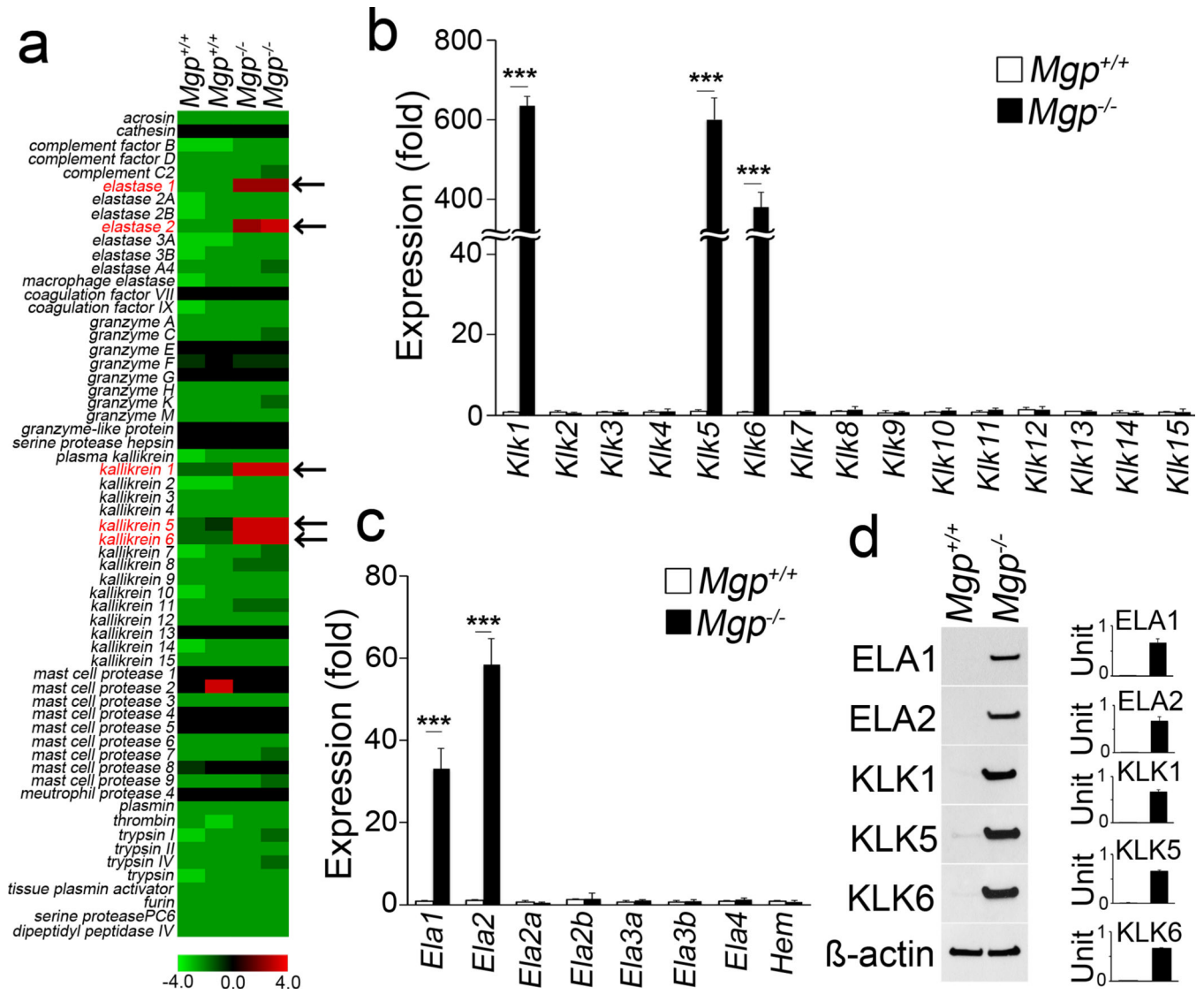


Figure 2. Activation of serine proteases in EndMTs and calcification

(a) Global gene expression profile of serine proteases in aortas from wild type (*Mgp*^{+/+}) and *Mgp*^{-/-} mice. (b–d) Expression of elastases (ELA) and kallikreins (KLK) in *Mgp*^{+/+} and *Mgp*^{-/-} aortas, determined by real-time PCR and immunoblotting with densitometry.

***p<0.001.

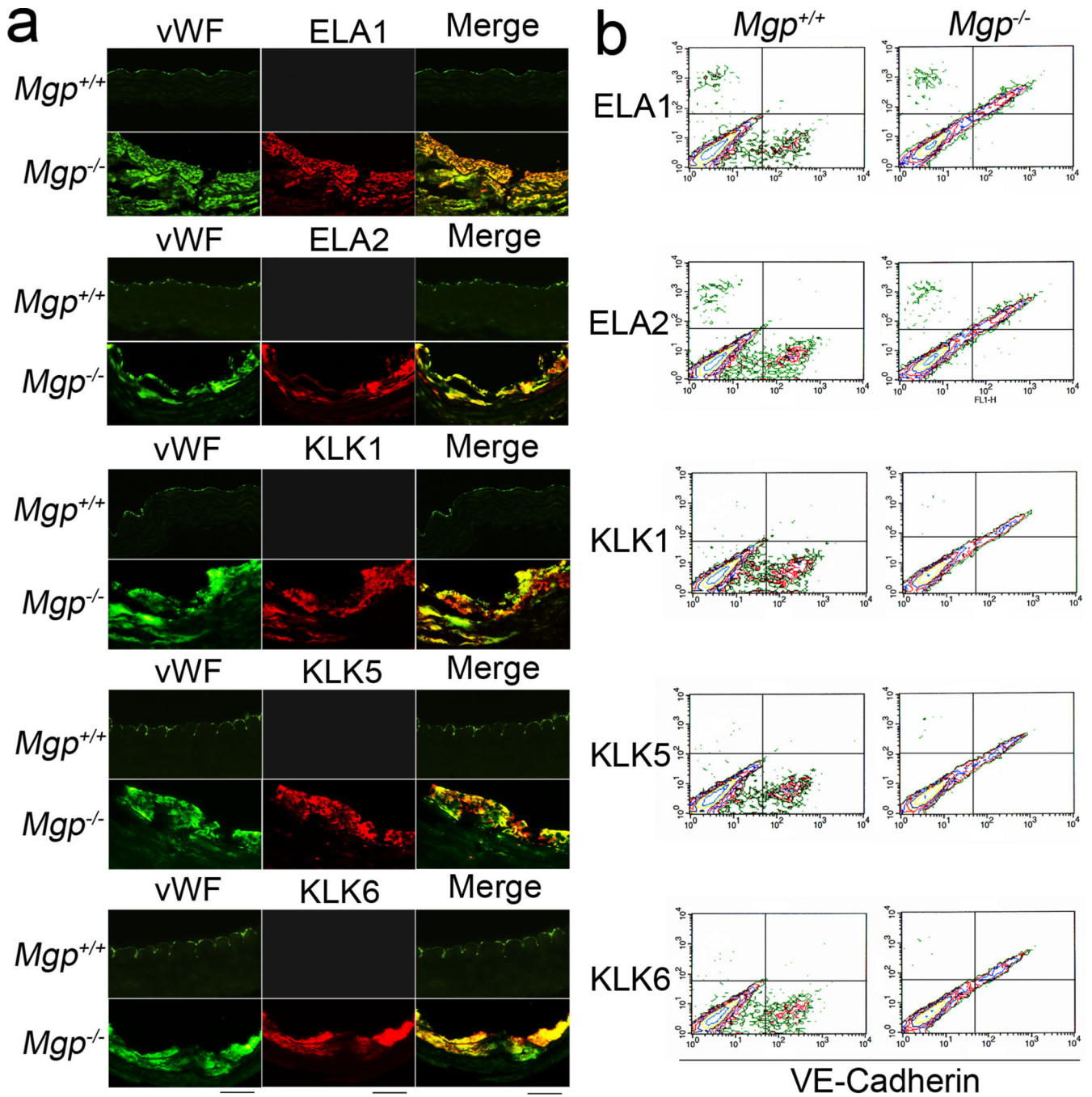


Figure 3. Induction of elastases and kallikreins in *Mgp*^{-/-} aortic endothelium
 (a) Immunostaining to detect co-localization of ELA 1, 2 and KLK 1, 5, 6 with the EC marker vWF. Scale bar: 100 μ m. (b) Flow cytometric analysis of co-expression of KLK 1, 5, 6 and VE-Cadherin in *Mgp*^{-/-} aortic cells.

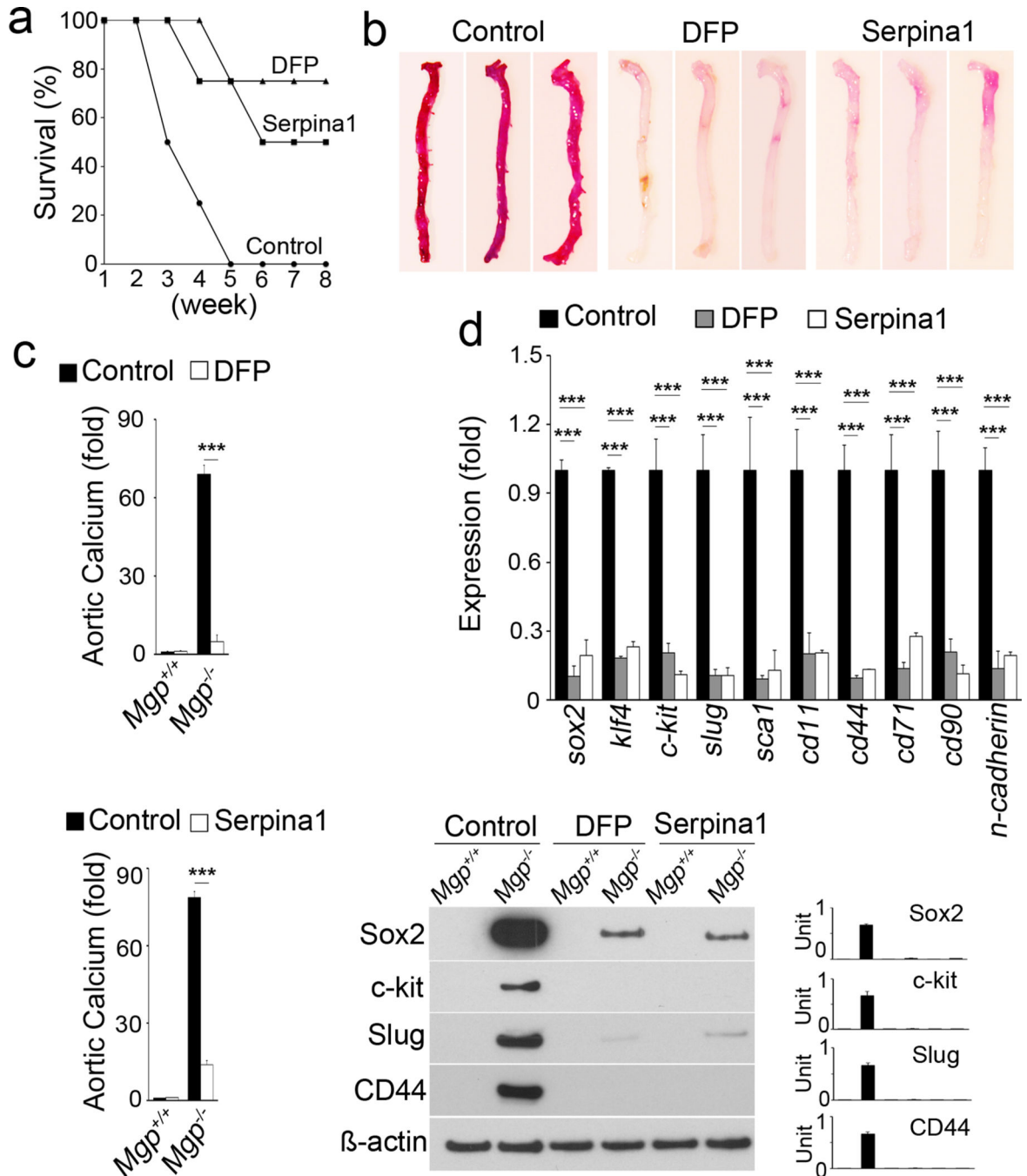


Figure 4. Inhibition of serine proteases decreases EndMTs and vascular calcification

(a) Survival rate of *Mgp*^{-/-} mice after treatment with DFP and serpin1 (n=8 per group). (b) Alizarin Red staining of *Mgp*^{-/-} aortas after 2 weeks of treatment with DFP or serpin1 injections. (c) Aortic calcium in *Mgp*^{-/-} aortas after injection of DFP (top) or serpin1 (bottom). ***p<0.001. (d) Expression of stem-cell markers in *Mgp*^{-/-} aortas after treatment with DFP or serpin1 as determined by real-time PCR (top) and immunoblotting with densitometry (bottom). ***p<0.001.

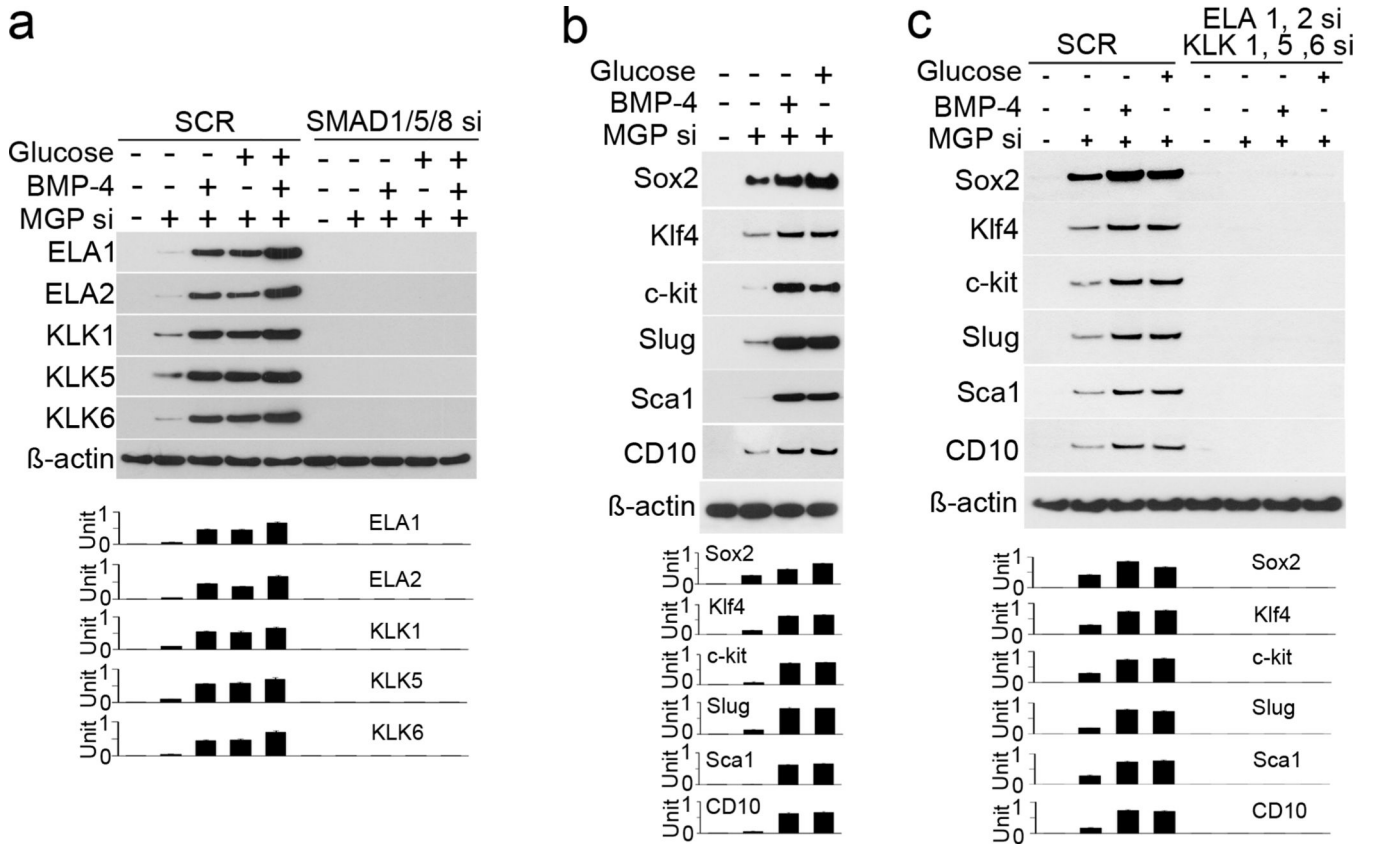


Figure 5. Elastases and kallikreins induce EndMTs in HAECs

(a) Elastase (ELA) 1, 2 and kallikrein (KLK) 1, 5, 6 were induced after depletion of MGP by siRNA (MGP si) in HAEC. The induction was enhanced by BMP-4 or high glucose, and abolished by transfection of siRNA to SMAD1/5/8 as shown by immunoblotting with densitometry. (b) Stem-cell and mesenchymal marker were induced after MGP si depletion in HAECs. The induction was enhanced by BMP-4 or high glucose as shown by immunoblotting with densitometry. (c) Depletion of elastase 1, 2 and kallikrein 1, 5, 6 by siRNA (si) abolished the induction of stem-cell markers in MGP-depleted HAECs as shown by immunoblotting with densitometry. SCR: scrambled siRNA.

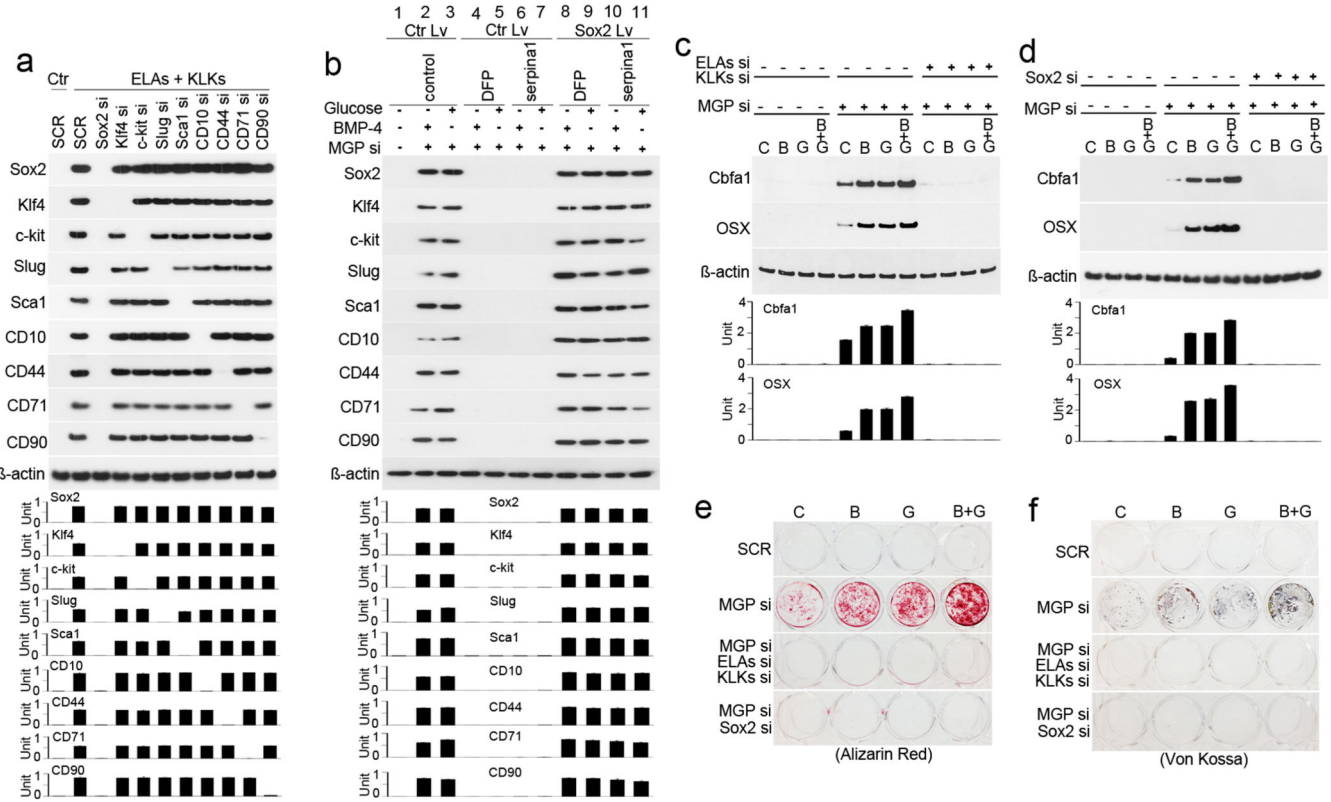


Figure 6. Sox2 mediates activation of elastases and kallikreins in the induction of EndMTs

(a) The expression of stem-cell markers was examined by immunoblotting with densitometry in HAECs treated with medium containing elastase 1, 2 (ELAs) and kallikrein 1, 5, 6 (KLKs), and transfected with siRNA (si) to each of the stem-cell markers individually. Ctr: control. SCR: scrambled siRNA. (b) HAECs were depleted of MGP by siRNA (si) and treated with high glucose and BMP-4, then treated with control (lane 1–3), DFP (lane 4–5), serpin1 (lane 6–7), or a combination of DFP, serpin1, and lentivirus (Lv) expressing Sox2 (lane 8–11). Expression of stem-cell markers was examined by immunoblotting with densitometry. (c–f) MGP-depleted HAECs were transfected with siRNAs (si) to elastase (ELA) 1, 2 and kallikrein (KLK) 1, 5, 6, or Sox2, and then treated with control (C), BMP-2 (B), glucose (G), or a combination. Expression of Cbfa1 and Osterix (OSX) was determined by immunoblotting with densitometry (c and d). Calcium accumulation was determined by Alizarin Red and Von Kossa staining (e and f). SCR: Scrambled siRNA.

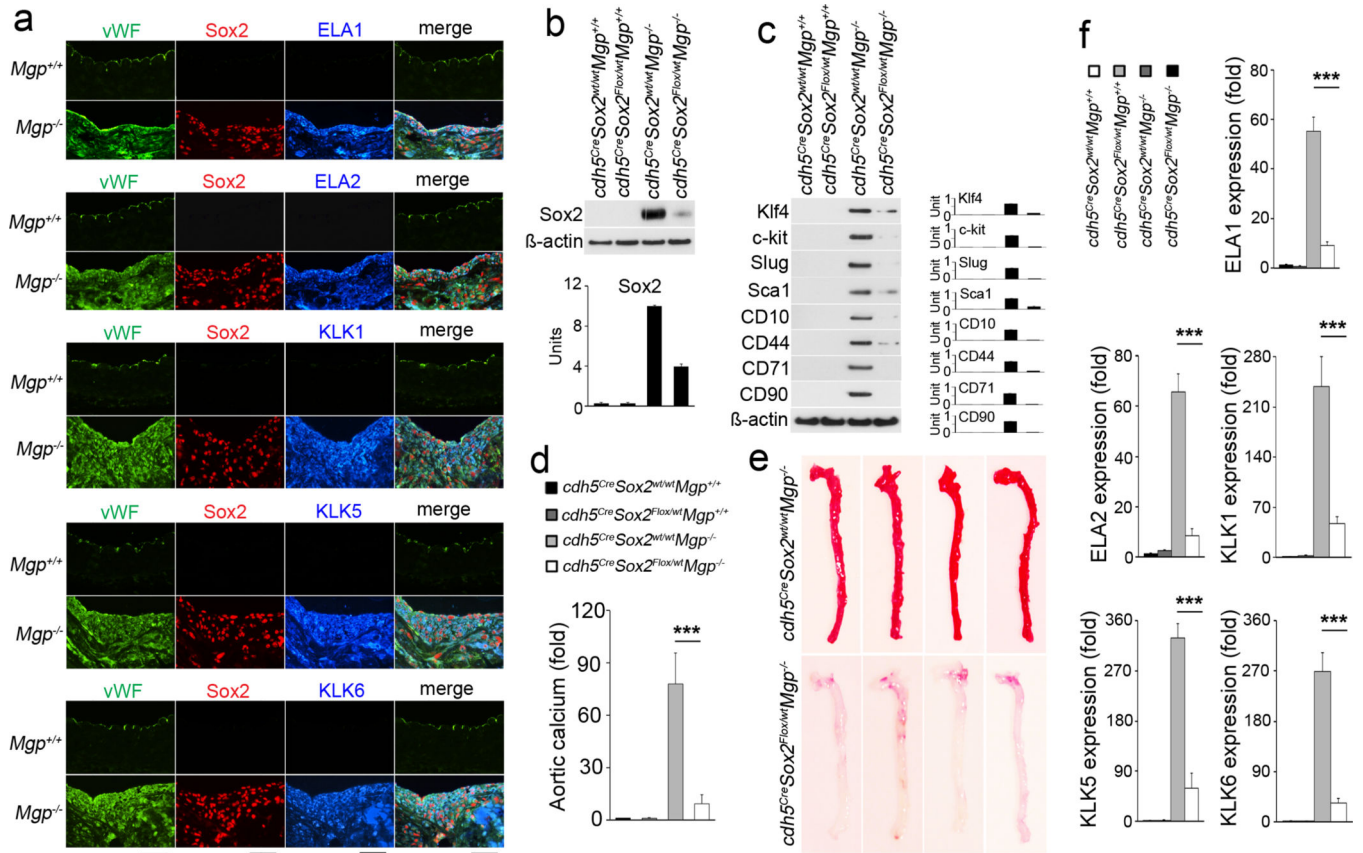


Figure 7. Limiting Sox2 in endothelium decreases EndMTs and calcification in *Mgp*^{-/-} aortas (a) Co-expression of elastase (ELA) 1, 2 and kallikrein (KLK) 1, 5, 6 with EC marker vWF and multipotency marker Sox2 in *Mgp*^{-/-} aortas as shown by immunostaining. Scale bars: 100 μ m. (b) Decreased expression of Sox2 in aortas of *Cdh5*^{Cre}*Sox2*^{Flox/wt}*Mgp*^{-/-}, as shown by immunoblotting with densitometry. (c) Decreased expression of stem-cell and mesenchymal markers in aortas of *Cdh5*^{Cre}*Sox2*^{Flox/wt}*Mgp*^{-/-}, as shown by immunoblotting with densitometry. (d) Aortic calcium in *Cdh5*^{Cre}*Sox2*^{wt/wt}*Mgp*^{-/-} and *Cdh5*^{Cre}*Sox2*^{Flox/wt}*Mgp*^{-/-} mice. ***p<0.001. (e) Alizarin Red staining of *Cdh5*^{Cre}*Sox2*^{wt/wt}*Mgp*^{-/-} and *Cdh5*^{Cre}*Sox2*^{Flox/wt}*Mgp*^{-/-} aortas. (f) Decrease of expression of elastase (ELA) 1, 2 and kallikrein (KLK) 1, 5, 6 in the in aortas of *Cdh5*^{Cre}*Sox2*^{Flox/wt}*Mgp*^{-/-}, as shown by real-time PCR. ***p<0.001.

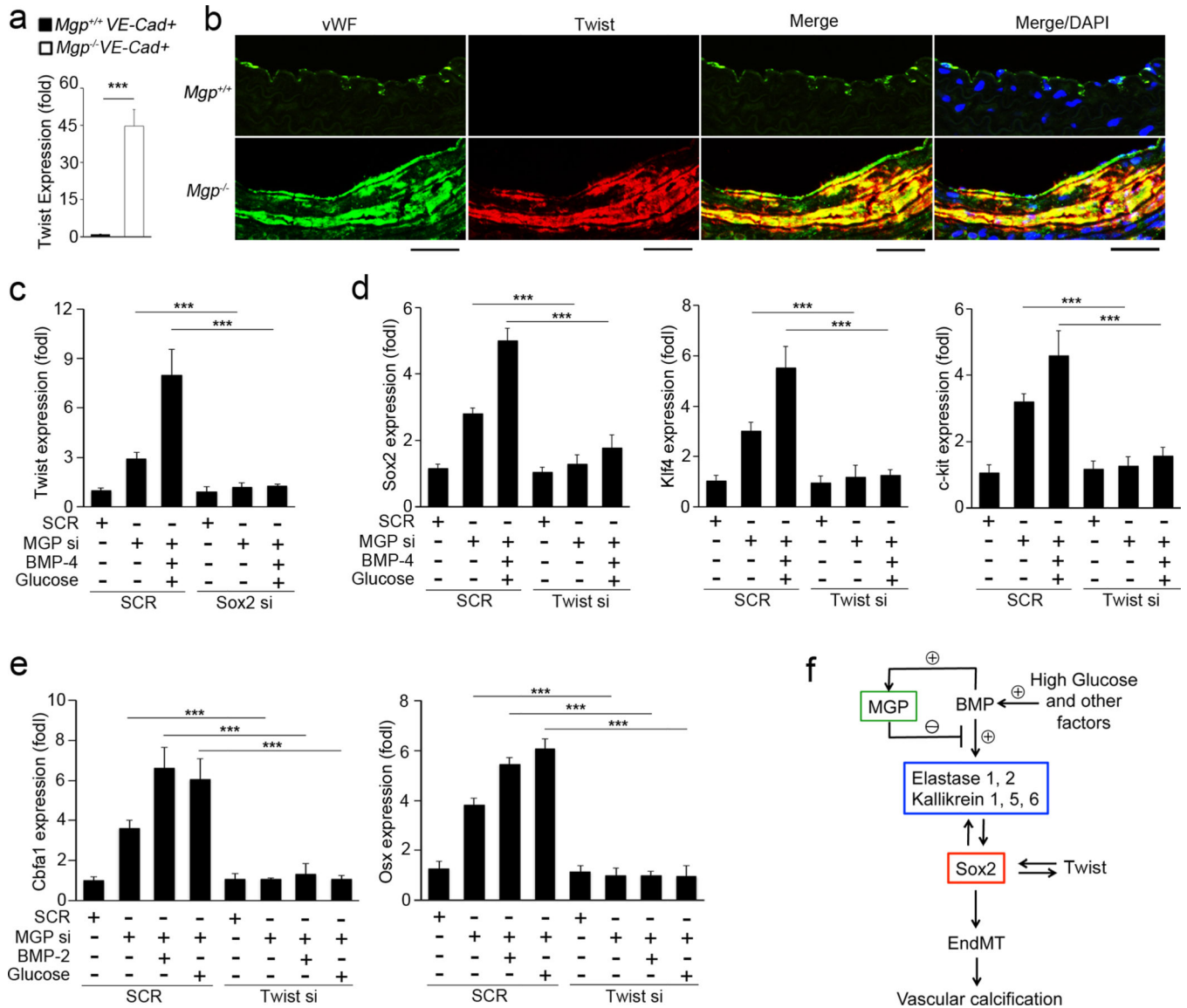


Figure 8. Mutual regulation of Sox2 and Twist1 in EndMTs in vascular calcification
 (a) Increase of Twist1 expression in VE-cadherin+CD45- presorted cells from *Mgp*^{-/-} aortas, as shown by real-time PCR. ***p<0.001. (b) Co-localization of Twist1 with the EC marker vWF in *Mgp*^{-/-} aortas, as shown by immunostaining. Scale bars: 100 μm. (c) MGP-depleted HAECs were transfected with siRNAs (si) to Sox2, and then treated with combinations of BMP-4 and glucose. Expression of Twist1 was examined by real-time PCR. ***p<0.001. (d) MGP-depleted HAECs were transfected with siRNAs (si) to Twist1, and then treated with combination of BMP-4 and glucose. Expression of Sox2, Klf4 and c-kit was examined by real-time PCR. ***p<0.001. (e) MGP-depleted HAECs were transfected with siRNAs (si) to Twist1, and then treated with BMP-2 or glucose for 4 days. Expression of Sox2, Klf4 and c-kit was examined by real-time PCR. ***p<0.001. (f) Schematic working model for the induction of serine proteases and Sox2 in EndMTs in vascular calcification.